EUROPEAN ORGANIZATION FOR NUCLEAR RESEARCH

CERN-EP/98-184
20 November 1998

χ_{c2} Formation in Two-Photon Collisions at LEP

The L3 Collaboration

Abstract

Two-photon formation of the charmonium resonance χ_{c2} has been studied with the L3 detector at LEP. The χ_{c2} is identified through its decay $\chi_{c2} \to \gamma J$, with a subsequent decay $J \to e^+e^-$ or $J \to \mu^+\mu^-$. With an integrated luminosity of 140 pb^{-1} at $\sqrt{s} \simeq 91$ GeV and 52 pb^{-1} at $\sqrt{s} \simeq 183$ GeV, we measure the two-photon width of the χ_{c2} to be

$$\Gamma_{\gamma\gamma}(\chi_{c2}) = 1.02 \pm 0.40 \text{ (stat.)} \pm 0.15 \text{ (sys.)} \pm 0.09\text{(BR.) keV}.$$

Submitted to *Phys. Lett. B*

Introduction

Several theoretical calculations of the partial decay widths of the charmonium $J^{PC} = 2^{++}$ meson χ_{c2} have been published [1–4]. In these models it is assumed that the two heavy quarks in the meson are bound together by a QCD potential. However, there are considerable differences in the treatment of the non-perturbative QCD effects and relativistic corrections. The models are also sensitive to input parameters such as the charm quark mass m_c, the value of the strong coupling constant $\alpha_s(m_c)$ and the shape of the quark potential. The predictions for the two-photon decay width of the χ_{c2} lie in the interval $0.3\ \text{keV} < \Gamma_{\gamma\gamma}(\chi_{c2}) < 0.6\ \text{keV}$.

More accurate predictions exist for the ratios between decay rates, such as $\Gamma_{\gamma\gamma}(\chi_{c0})/\Gamma_{\gamma\gamma}(\chi_{c2})$ [5] or the ratio of the two-gluon width to the two-photon width $\Gamma_{gg}(\chi_{c2})/\Gamma_{\gamma\gamma}(\chi_{c2})$ [6–8], since the relativistic corrections and the dependence on the quark potential cancel. In next-to-leading order one obtains for the latter ratio [6]

$$\frac{\Gamma_{gg}(\chi_{c2})}{\Gamma_{\gamma\gamma}(\chi_{c2})} = \frac{9{\alpha_s}^2(m_c)}{8\alpha^2}\left(\frac{1-2.2\alpha_s/\pi}{1-16\alpha_s/3\pi}\right). \tag{1}$$

For $\Gamma_{gg}(\chi_{c2})$ one can take either $\Gamma(\chi_{c2} \to \text{hadrons})$, or, according to reference [7], the difference $\Gamma(\chi_{c2} \to \text{hadrons}) - \Gamma(\chi_{c1} \to \text{hadrons})$. Here, the term $\Gamma(\chi_{c1} \to \text{hadrons})$ is assumed to be equal to the three-gluon width of the χ_{c2}, since the χ_{c1} can only decay to hadrons through a three-gluon decay, and the χ_{c1} and the χ_{c2} are close in mass. Equation (1) can be used to determine $\alpha_s(m_c)$ from a measurement of $\Gamma_{\gamma\gamma}(\chi_{c2})$ [9].

At e^+e^- colliders, two-photon interactions are studied via the process $e^+e^- \to e^+e^-\gamma\gamma \to e^+e^-X$. The scattered electron and positron carry almost the full beam energy and usually escape undetected (untagged events). If the scattering angle is sufficiently large, they can be detected in the forward electromagnetic calorimeters (tagged events). If the final state X is a resonance R, it must have positive charge conjugation and the total production cross section is given by

$$\sigma(e^+e^- \to e^+e^-R) = \int \mathrm{d}^5 L_{\gamma\gamma}\ \sigma(\gamma\gamma \to R). \tag{2}$$

Here, $L_{\gamma\gamma}$ is the two-photon luminosity function described by QED [10], and $\sigma(\gamma\gamma \to R)$ is, for quasi-real photons, given by the Breit-Wigner formula

$$\sigma(\gamma\gamma \to R) = 8\pi(2J_R+1)\frac{\Gamma_{\gamma\gamma}(R)\Gamma_R}{(W_{\gamma\gamma}^2 - m_R^2)^2 + m_R^2\Gamma_R^2}, \tag{3}$$

where $W_{\gamma\gamma}$ is the two-photon invariant mass, and m_R, J_R, $\Gamma_{\gamma\gamma}(R)$ and Γ_R are the mass, spin, two-photon decay width and total decay width of the resonance R, respectively. Equations (2) and (3) show that there is a linear relationship between the total cross section $\sigma(e^+e^- \to e^+e^-R)$ and the two-photon decay width $\Gamma_{\gamma\gamma}(R)$.

We identify the χ_{c2} through its decay into γJ, with $J \to e^+e^-$ or $\mu^+\mu^-$. The total branching ratio for $\chi_{c2} \to e^+e^-\gamma$ or $\mu^+\mu^-\gamma$ is BR=0.0162±0.0014 [11]. In this decay mode, the sensitivity to χ_{c1} and χ_{c0} formation is small, because the branching ratio $\chi_{c0} \to \gamma J \to e^+e^-\gamma$ or $\mu^+\mu^-\gamma$ is $(8\pm2)\cdot10^{-4}$ [11], and χ_{c1} production by two real photons is forbidden by the Landau-Yang theorem [12].

L3 detector

A detailed description of the L3 detector can be found elsewhere [13]. This analysis uses the Silicon Microvertex Detector and the Time Expansion Chamber (TEC) for the tracking of

charged particles, and the Electromagnetic Calorimeter (ECAL), consisting of BGO crystals, to detect photons and identify electrons and muons. The scattered beam electrons may be detected in the forward Luminosity Monitor (LUMI), also consisting of BGO crystals. Until 1995, the tagging acceptance of the LUMI was 26 mrad$< \theta <$ 65 mrad, where θ is the polar angle with respect to the incident beams. From 1996 onwards, it is decreased to 30 mrad$< \theta <$65 mrad due to the installation of a radiation shield. Since 1996, the scattered beam electrons can also be detected in a Very Small Angle Tagger (VSAT) [14]. This detector consists of four units each containing 24 BGO crystals, positioned in the horizontal plane behind the first LEP quadrupole magnets at 8.2 m from the interaction point. The VSAT acceptance is 5 mrad$< \theta <$ 8 mrad for -0.8 rad$< \phi <$ 0.8 rad and π-0.8 rad$< \phi < \pi +$ 0.8 rad, where ϕ is the azimuthal angle and ϕ=0 corresponds to the plane of the LEP ring.

Data analysis

We analyse data taken in the years 1991 to 1995 at centre-of-mass energies around 91 GeV corresponding to an integrated luminosity of 140.2 pb^{-1} (LEP1 data), and data taken in 1997 at $\sqrt{s} \simeq 183$ GeV corresponding to 52.4 pb^{-1} (LEP2 data).

In order to select $\chi_{c2} \to \gamma$J, J $\to e^+e^-$ or $\mu^+\mu^-$ events, the following selection criteria are applied:

- The event must have two tracks of opposite charge and with transverse momenta 0.05 GeV$< p_t <$ 15 GeV. A track must have at least 12 out of a maximum of 62 hits in the TEC, and the distance between the first and last hit should be at least 15 wires. The distance of closest approach to the beam line in the transverse plane is required to be smaller than 2 mm.

- Electrons and muons are identified using their signatures in the ECAL. Since the electrons leave all their energy in the calorimeter, the energy E measured in the ECAL must be close to the track momentum p. To identify the electron pair, we require for one track $0.9 < E/p < 1.1$ and for the other track $0.7 < E/p < 1.3$. Muons with momenta smaller than 2 GeV do not reach the muon chambers. They are identified by their minimum ionising signature in the ECAL, corresponding to an energy deposition of less than 0.45 GeV.

- The event should have one photon. A photon candidate is defined as an electromagnetic cluster in the ECAL, separated from both tracks by at least 100 mrad in ϕ and 140 mrad in θ. Since the χ_{c2} decay photon typically has an energy around 0.46 GeV, a cut requiring $E_\gamma >$0.3 GeV is very efficient in reducing the background, as shown in Figure 1.

- To reject radiative events of the type $e^+e^- \to e^+e^-e^+e^-\gamma$, the photon should not be close to either one of the tracks in the centre-of-mass system of the χ_{c2}; therefore, if $\cos\theta(\ell,\gamma) > 0.96$, the event is rejected.

- If a cluster with energy $E > 0.7\ E_{\rm beam}$ is found in the LUMI calorimeter, or a cluster of $E > 0.5\ E_{\rm beam}$ is detected in the VSAT calorimeter, the event is classified as tagged.

- To select exclusive final states, the squared vectorial sum of the transverse momentum $\vec{p}_t$ of all measured particles, $(\Sigma\vec{p}_t)^2$, is required to be small. If a tag is found it is also included in the sum. However, if $(\Sigma\vec{p}_t)^2$ excluding the $\vec{p}_t$ of the tag is smaller than the $(\Sigma\vec{p}_t)^2$ with the tag included, the event is regarded as untagged. For untagged events and

events with a LUMI tag, we require $(\Sigma\vec{p}_{\rm t})^2 < 0.08$ GeV^2, while for events with a VSAT tag, we cut at $(\Sigma\vec{p}_{\rm t})^2 < 0.1$ GeV^2.

- Finally, a cut is made on the invariant mass of the lepton pair $M(\ell^+\ell^-)$. For LEP1 data, we cut at $|M(\ell^+\ell^-) - M({\rm J})| < 0.25$ GeV. For LEP2 data the resolution is slightly worse because the tracks are on average at smaller polar angles; therefore the cut is loosened to 0.30 GeV.

Figure 2 shows the mass difference $\Delta M = M(\ell^+\ell^-\gamma) - M(\ell^+\ell^-)$ for the events passing all cuts described above. The hatched areas represent single-tagged events. A peak is observed at the position expected for the $\chi_{\rm c2}$: $\Delta M = M(\chi_{\rm c2}) - M({\rm J}) = 0.459$ GeV.

Selection efficiency

The selection efficiency is determined with a Monte Carlo program [15] which generates the $e^+e^- \to e^+e^-\chi_{\rm c2}$, $\chi_{\rm c2} \to \gamma{\rm J}$ events according to the luminosity function of Reference [10]. We include only the contribution of two transversely polarised photons. The explicit Q^2-dependence of the cross section, where $-Q^2$ is the invariant mass squared of the virtual photon, is taken into account by multiplying the cross section with a Vector Meson Dominance (VMD) transition form factor with a J pole:

$$\sigma \sim \left(\frac{1}{1+Q_1^2/M({\rm J})^2}\right)^2 \left(\frac{1}{1+Q_2^2/M({\rm J})^2}\right)^2 \tag{4}$$

We assume that only the helicity state $|\lambda| = 2$ contributes to $\gamma\gamma \to \chi_{\rm c2}$ formation [1,5]. The $\chi_{\rm c2}$ decay products are generated according to a phase space distribution, *i.e.* uniform in $\cos\theta^*$, ϕ^*, $\cos\theta'$, and ϕ'. Here, θ^* and ϕ^* are the polar and azimuthal angles of the photon relative to the photon-photon collision axis in the $\chi_{\rm c2}$ centre-of-mass frame, and θ' and ϕ' define the e^+ or μ^+ direction in the J rest frame. θ' is the angle between the positive lepton and the direction of flight of the J, while ϕ' is the angle between the production and decay planes of the J. In order to correct for the dependence of the angular distribution on the helicity of the spin-two resonance, each Monte Carlo event is weighted with a function $f_\lambda(\theta^*, \theta', \phi')$ [16,17]:

$$\begin{aligned} f_\lambda(\theta^*,\theta',\phi') &= \frac{1}{8}A_2^2(1+\cos^2\theta')(1+6\cos^2\theta^*+\cos^4\theta^*) \\ &+ A_1^2(1-\cos^2\theta')(1-\cos^4\theta^*) \\ &+ \frac{3}{4}A_0^2(1+\cos^2\theta')(1-2\cos^2\theta^*+\cos^4\theta^*) \\ &+ \frac{1}{4}\sqrt{2}A_2A_1\cos\phi'\sin 2\theta'\sin\theta^*(\cos^3\theta^*+3\cos\theta^*) \\ &+ \frac{1}{4}\sqrt{6}A_2A_0\cos 2\phi'\sin^2\theta'(1-\cos^4\theta^*) \\ &- \frac{1}{2}\sqrt{3}A_1A_0\cos\phi'\sin 2\theta'\sin^3\theta^*\cos\theta^*. \end{aligned} \tag{5}$$

The decay amplitudes A_0, A_1, and A_2 have been measured [18] to be 0.21±0.03, 0.49±0.07, and 0.85±0.05, respectively. Using a pure electric dipole transition would result in coefficients $A_0 = 0.316$, $A_1 = 0.549$, and $A_2 = 0.775$. This alternative is taken into account in the determination of the systematic error.

All generated events are passed through a full detector simulation and are reconstructed following the same procedure as used for the data [19]. A trigger simulation is also included. Most events are triggered by the charged track trigger, which requires two acoplanar tracks, but some are also triggered by the calorimeter trigger. In addition, there is a trigger for electron tags in the LUMI calorimeter. The trigger efficiency for untagged events for LEP1 data is 88±4%, while for LEP2 data it is 89±5%.

The total efficiency, including the detector acceptance, for untagged data is 10.4±0.5% at LEP1, while at LEP2 it is 8.6±0.5%. At LEP2, the acceptance is somewhat lower due to the larger average boost of the χ_{c2} system.

Results

Only the untagged events are used for the measurement of $\Gamma_{\gamma\gamma}(\chi_{c2})$. They are plotted in Figure 3a. In Figure 3b the ΔM spectrum for the J sidebands (2.45 GeV $< M(\ell^+\ell^-) <$ 2.75 GeV and 3.45 GeV $< M(\ell^+\ell^-) <$ 3.75 GeV) is shown. The sideband events for LEP1 data and LEP2 data have been added together. This spectrum describes the shape of the background under the χ_{c2} signal. It is parametrised by a threshold function

$$b(x) = a_1 \frac{\exp(-x/a_2)}{1+\exp((a_3-x)/a_4)}, \tag{6}$$

where a_1 is chosen such that $b(x)$ is normalised to one. The J sideband spectrum, the LEP1 spectrum and the LEP2 spectrum are fitted simultaneously in an unbinned likelihood fit. In this way the statistical uncertainty of the background is automatically included in the fit. The J sideband spectrum is fitted with the threshold function $b(x)$. The LEP1 and LEP2 data spectra are each fitted with a sum of the threshold function and a Gaussian distribution $g(x)$:

$$f_i(x) = (1-p_i)\, b(x) + p_i\, g(x) \tag{7}$$

Here, p_i is the ratio of the number of signal events S_i over the number of total events N_i in data spectrum i. The parameters of the threshold function a_2, a_3, and a_4, and the position and the width of the Gaussian distribution are required to be the same for all spectra. The number of signal events in the LEP1 and LEP2 samples, S_1 and S_2, are both related to the two-photon width by the relation

$$S_i = \epsilon_i\, L_i\, BR\, \kappa_i\, \Gamma_{\gamma\gamma}. \tag{8}$$

Here, ϵ_i is the total efficiency for data sample i, L_i the integrated luminosity, and BR the branching ratio $\chi_{c2} \to \gamma e^+e^-$ or $\gamma\mu^+\mu^-$. The factor κ_i, relating the cross section to the two-photon width, is obtained from Monte Carlo.

The curves in Figure 3 show the fitted signal and background functions. The fit gives for the position of the χ_{c2} signal ΔM=0.445±0.010 GeV, in agreement with the expected position. Also the width, $\sigma(\Delta M)$=0.023±0.007 GeV, due entirely to to the experimental resolution, agrees with the Monte Carlo expectations. The 13.6 signal events obtained from the fit correspond to a two-photon width of $\Gamma_{\gamma\gamma}(\chi_{c2}) = 1.02 \pm 0.40$ (stat.) keV.

The systematic error due to a variation of the cut on the photon energy from 0.275 to 0.325 GeV is 7%. If the cut on $M(\ell^+\ell^-)$ is varied by 0.05 GeV in both directions, the two-photon width changes by 11%. Variations of the other selection cuts give much smaller contributions to the systematic error, and are neglected. The uncertainties in the trigger efficiency result in

a 4% uncertainty on the value of $\Gamma_{\gamma\gamma}(\chi_{c2})$. Changing the VMD J pole form factor to a VMD ρ pole form factor increases the two-photon width by 4%. A 5% helicity-zero contribution to $\gamma\gamma \to \chi_{c2}$ formation would decrease the two-photon width by 1%. Varying the decay amplitudes in equation (5) within their errors results in a 2% error. Taking an electric dipole transition for these amplitudes also gives a 2% contribution to the error. We assume that the error due to taking into account only the transverse-transverse two-photon cross section can be neglected.

The different contributions to the systematic error are summarised in Table 1. They result in a total systematic error of 15%. The systematic error due to the uncertainty on the branching ratio $\chi_{c2} \to e^+e^-\gamma$ or $\mu^+\mu^-\gamma$ is 8% [11]. The final value for the two-photon width of the χ_{c2} is therefore

$$\Gamma_{\gamma\gamma}(\chi_{c2}) = 1.02 \pm 0.40\ (\text{stat.}) \pm 0.15\ (\text{sys.}) \pm 0.09(\text{BR.})\ \text{keV}. \tag{9}$$

In Figure 2, the tagged events are also shown. At $\sqrt{s} \simeq 91$ GeV, we observe one χ_{c2} candidate with a tag in the Luminosity Monitor ($1\ \text{GeV}^2 < Q^2 < 9\ \text{GeV}^2$), with an estimated background of 0.8 events. For a VMD form factor with a J pole, we would expect 0.95 signal events, while for a VMD form factor with a ρ pole, we would expect 0.05. At $\sqrt{s} \simeq 183$ GeV we find one candidate event with a tag in the VSAT ($0.1\ \text{GeV}^2 < Q^2 < 0.9\ \text{GeV}^2$), with negligible background. Here we expect 0.14 events in case of a J pole and 0.06 events in case of a ρ pole. This is the first indication of tagged χ_{c2} events. The confidence levels for a J pole and a ρ pole form factor are 27% and 16%, respectively. Due to the low statistics and the unknown contribution of the χ_{c1} background in these Q^2 intervals, it is not yet possible to measure the χ_{c2} transition form factor.

Using equation (1) the $\Gamma_{\gamma\gamma}(\chi_{c2})$ measurement can be converted into a measurement of $\alpha_s(m_c)$. With $\Gamma_{gg}(\chi_{c2}) = \Gamma(\chi_{c2} \to \text{hadrons}) = 1.73 \pm 0.21$ MeV [11], and α=1/137, we obtain $\alpha_s(m_c) = 0.25 \pm 0.06$. If we use $\Gamma_{gg}(\chi_{c2}) = \Gamma(\chi_{c2} \to \text{hadrons}) - \Gamma(\chi_{c1} \to \text{hadrons})$, with $\Gamma(\chi_{c1} \to \text{hadrons}) = 0.64 \pm 0.11$ MeV [11], we obtain $\alpha_s(m_c) = 0.21 \pm 0.05$. These values are lower than the measurements obtained at the τ mass, $\alpha_s(m_\tau) = 0.334 \pm 0.022$ [20]. The latter is consistent with α_s values measured in Z-decays evolved to the charm mass ($m_\tau \simeq m_c$). Similar discrepancies have been observed in other α_s determinations from the decays of $c\bar{c}$ and $b\bar{b}$ states [8, 9].

In Table 2, our value of $\Gamma_{\gamma\gamma}(\chi_{c2})$ is compared to previous measurements [21–25]. Within errors, the agreement is good. However, the combined value of all two-photon measurements, $\Gamma_{\gamma\gamma}(\chi_{c2}) = 1.23 \pm 0.23(\text{stat.} + \text{sys.}) \pm 0.11(\text{BR.})$ keV, is three standard deviations higher than the $p\bar{p}$ measurement of E760. The theoretical predictions [1–4] are also listed in Table 2. Our measurement is somewhat higher than these predictions, but it agrees within errors.

Acknowledgements

We would like to thank G. Schuler for his calculation of the angular distributions of the χ_{c2}, and for helpful discussions. We wish to express our gratitude to the CERN accelerator division for the excellent performance of the LEP machine. We acknowledge the contributions of all the engineers and technicians who have participated in the construction and maintenance of this experiment.

Author List

The L3 Collaboration:

M.Acciarri,[26] P.Achard,[18] O.Adriani,[15] M.Aguilar-Benitez,[25] J.Alcaraz,[25] G.Alemanni,[21] J.Allaby,[16] A.Aloisio,[28] M.G.Alviggi,[28] G.Ambrosi,[18] H.Anderhub,[47] V.P.Andreev,[6,36] T.Angelescu,[12] F.Anselmo,[9] A.Arefiev,[27] T.Azemoon,[3] T.Aziz,[10] P.Bagnaia,[35] L.Baksay,[42] A.Balandras,[4] R.C.Ball,[3] S.Banerjee,[10] Sw.Banerjee,[10] K.Banicz,[44] A.Barczyk,[47,45] R.Barillère,[16] L.Barone,[35] P.Bartalini,[21] M.Basile,[9] R.Battiston,[32] A.Bay,[21] F.Becattini,[15] U.Becker,[14] F.Behner,[47] J.Berdugo,[25] P.Berges,[14] B.Bertucci,[32] B.L.Betev,[47] S.Bhattacharya,[10] M.Biasini,[32] A.Biland,[47] J.J.Blaising,[4] S.C.Blyth,[33] G.J.Bobbink,[2] R.Bock,[1] A.Böhm,[1] L.Boldizsar,[13] B.Borgia,[16,35] D.Bourilkov,[47] M.Bourquin,[18] S.Braccini,[18] J.G.Branson,[38] V.Brigljevic,[47] F.Brochu,[4] A.Buffini,[15] A.Buijs,[43] J.D.Burger,[14] W.J.Burger,[32] J.Busenitz,[42] A.Button,[3] X.D.Cai,[14] M.Campanelli,[47] M.Capell,[14] G.Cara Romeo,[9] G.Carlino,[28] A.M.Cartacci,[15] J.Casaus,[25] G.Castellini,[15] F.Cavallari,[35] N.Cavallo,[28] C.Cecchi,[18] M.Cerrada,[25] F.Cesaroni,[22] M.Chamizo,[25] Y.H.Chang,[49] U.K.Chaturvedi,[17] M.Chemarin,[24] A.Chen,[49] G.Chen,[7] G.M.Chen,[7] H.F.Chen,[19] H.S.Chen,[7] X.Chereau,[4] G.Chiefari,[28] L.Cifarelli,[37] F.Cindolo,[9] C.Civinini,[15] I.Clare,[14] R.Clare,[14] G.Coignet,[4] A.P.Colijn,[2] N.Colino,[25] S.Costantini,[8] F.Cotorobai,[12] B.de la Cruz,[25] A.Csilling,[13] T.S.Dai,[14] J.A.van Dalen,[30] R.D'Alessandro,[15] R.de Asmundis,[28] P.Deglon,[18] A.Degré,[4] K.Deiters,[45] D.della Volpe,[28] P.Denes,[34] F.DeNotaristefani,[35] A.De Salvo,[47] M.Diemoz,[35] D.van Dierendonck,[2] F.Di Lodovico,[47] C.Dionisi,[16,35] M.Dittmar,[47] A.Dominguez,[38] A.Doria,[28] M.T.Dova,[17,♯] D.Duchesneau,[4] D.Dufournand,[4] P.Duinker,[2] I.Duran,[39] H.El Mamouni,[24] A.Engler,[33] F.J.Eppling,[14] F.C.Erné,[2] P.Extermann,[18] M.Fabre,[45] R.Faccini,[35] M.A.Falagan,[25] S.Falciano,[35] A.Favara,[15] J.Fay,[24] O.Fedin,[36] M.Felcini,[47] T.Ferguson,[33] F.Ferroni,[35] H.Fesefeldt,[1] E.Fiandrini,[32] J.H.Field,[18] F.Filthaut,[16] P.H.Fisher,[14] I.Fisk,[38] G.Forconi,[14] L.Fredj,[18] K.Freudenreich,[47] C.Furetta,[26] Yu.Galaktionov,[27,14] S.N.Ganguli,[10] P.Garcia-Abia,[5] M.Gataullin,[31] S.S.Gau,[11] S.Gentile,[35] N.Gheordanescu,[12] S.Giagu,[35] S.Goldfarb,[21] Z.F.Gong,[19] M.W.Gruenewald,[8] R.van Gulik,[2] V.K.Gupta,[34] A.Gurtu,[10] L.J.Gutay,[44] D.Haas,[5] B.Hartmann,[1] A.Hasan,[29] D.Hatzifotiadou,[9] T.Hebbeker,[8] A.Hervé,[16] P.Hidas,[13] J.Hirschfelder,[33] H.Hofer,[47] G. Holzner,[47] H.Hoorani,[33] S.R.Hou,[49] I.Iashvili,[46] B.N.Jin,[7] L.W.Jones,[3] P.de Jong,[16] I.Josa-Mutuberría,[25] R.A.Khan,[17] D.Kamrad,[46] J.S.Kapustinsky,[23] M.Kaur,[17,◇] M.N.Kienzle-Focacci,[18] D.Kim,[35] D.H.Kim,[41] J.K.Kim,[41] S.C.Kim,[41] W.W.Kinnison,[23] J.Kirkby,[16] D.Kiss,[13] W.Kittel,[30] A.Klimentov,[14,27] A.C.König,[30] A.Kopp,[46] I.Korolko,[27] V.Koutsenko,[14,27] R.W.Kraemer,[33] W.Krenz,[1] A.Kunin,[14,27] P.Lacentre,[46,♮,♯] P.Ladron de Guevara,[25] I.Laktineh,[24] G.Landi,[15] C.Lapoint,[14] K.Lassila-Perini,[47] P.Laurikainen,[20] A.Lavorato,[37] M.Lebeau,[16] A.Lebedev,[14] P.Lebrun,[24] P.Lecomte,[47] P.Lecoq,[16] P.Le Coultre,[47] H.J.Lee,[8] J.M.Le Goff,[16] R.Leiste,[46] E.Leonardi,[35] P.Levtchenko,[36] C.Li,[19] C.H.Lin,[49] W.T.Lin,[49] F.L.Linde,[2,16] L.Lista,[28] Z.A.Liu,[7] W.Lohmann,[46] E.Longo,[35] Y.S.Lu,[7] K.Lübelsmeyer,[1] C.Luci,[16,35] D.Luckey,[14] L.Luminari,[35] W.Lustermann,[47] W.G.Ma,[19] M.Maity,[10] G.Majumder,[10] L.Malgeri,[16] A.Malinin,[27] C.Maña,[25] D.Mangeol,[30] P.Marchesini,[47] G.Marian,[42,¶] J.P.Martin,[24] F.Marzano,[35] G.G.G.Massaro,[2] K.Mazumdar,[10] R.R.McNeil,[6] S.Mele,[16] L.Merola,[28] M.Meschini,[15] W.J.Metzger,[30] M.von der Mey,[1] D.Migani,[9] A.Mihul,[12] H.Milcent,[16] G.Mirabelli,[35] J.Mnich,[16] P.Molnar,[8] B.Monteleoni,[15] T.Moulik,[10] G.S.Muanza,[24] F.Muheim,[18] A.J.M.Muijs,[2] S.Nahn,[14] M.Napolitano,[28] F.Nessi-Tedaldi,[47] H.Newman,[31] T.Niessen,[1] A.Nippe,[21] A.Nisati,[35] H.Nowak,[46] Y.D.Oh,[41] G.Organtini,[35] R.Ostonen,[20] C.Palomares,[25] D.Pandoulas,[1] S.Paoletti,[35,16] P.Paolucci,[28] H.K.Park,[33] I.H.Park,[41] G.Pascale,[35] G.Passaleva,[16] S.Patricelli,[28] T.Paul,[11] M.Pauluzzi,[32] C.Paus,[16] F.Pauss,[47] D.Peach,[16] M.Pedace,[35] Y.J.Pei,[1] S.Pensotti,[26] D.Perret-Gallix,[4] B.Petersen,[30] S.Petrak,[8] D.Piccolo,[28] M.Pieri,[15] P.A.Piroué,[34] E.Pistolesi,[26] V.Plyaskin,[27] M.Pohl,[47] V.Pojidaev,[27,15] H.Postema,[14] J.Pothier,[16] N.Produit,[18] D.Prokofiev,[36] J.Quartieri,[37] G.Rahal-Callot,[47] N.Raja,[10] P.G.Rancoita,[26] G.Raven,[38] P.Razis,[29] D.Ren,[47] M.Rescigno,[35] S.Reucroft,[11] T.van Rhee,[43] S.Riemann,[46] K.Riles,[3] A.Robohm,[47] J.Rodin,[42] B.P.Roe,[3] L.Romero,[25] S.Rosier-Lees,[4] S.Roth,[1] J.A.Rubio,[16] D.Ruschmeier,[8] H.Rykaczewski,[47] S.Sakar,[35] J.Salicio,[16] E.Sanchez,[25] M.P.Sanders,[30] M.E.Sarakinos,[20] C.Schäfer,[1] V.Schegelsky,[36] S.Schmidt-Kaerst,[1] D.Schmitz,[1] N.Scholz,[47] H.Schopper,[48] D.J.Schotanus,[30] J.Schwenke,[1] G.Schwering,[1] C.Sciacca,[28] D.Sciarrino,[18] L.Servoli,[32] S.Shevchenko,[31] N.Shivarov,[40] V.Shoutko,[27] J.Shukla,[23] E.Shumilov,[27] A.Shvorob,[31] T.Siedenburg,[1] D.Son,[41] B.Smith,[33] P.Spillantini,[15] M.Steuer,[14] D.P.Stickland,[34] A.Stone,[6] H.Stone,[34] B.Stoyanov,[40] A.Straessner,[1] K.Sudhakar,[10] G.Sultanov,[17] L.Z.Sun,[19] H.Suter,[47] J.D.Swain,[17] Z.Szillasi,[42,¶] X.W.Tang,[7] L.Tauscher,[5] L.Taylor,[11] C.Timmermans,[30] Samuel C.C.Ting,[14] S.M.Ting,[14] S.C.Tonwar,[10] J.Tóth,[13] C.Tully,[34] K.L.Tung,[7] Y.Uchida,[14] J.Ulbricht,[47] E.Valente,[35] G.Vesztergombi,[13] I.Vetlitsky,[27] G.Viertel,[47] S.Villa,[11] M.Vivargent,[4] S.Vlachos,[5] H.Vogel,[33] H.Vogt,[46] I.Vorobiev,[16,27] A.A.Vorobyov,[36] A.Vorvolakos,[29] M.Wadhwa,[5] W.Wallraff,[1] J.C.Wang,[14] X.L.Wang,[19] Z.M.Wang,[19] A.Weber,[1] H.Wilkens,[30] S.X.Wu,[14] S.Wynhoff,[1] L.Xia,[31] Z.Z.Xu,[19] B.Z.Yang,[19] C.G.Yang,[7] H.J.Yang,[7] M.Yang,[7] J.B.Ye,[19] S.C.Yeh,[50] J.M.You,[33] An.Zalite,[36] Yu.Zalite,[36] P.Zemp,[47] Y.Zeng,[1] Z.P.Zhang,[19] G.Y.Zhu,[7] R.Y.Zhu,[31] A.Zichichi,[9,16,17] F.Ziegler,[46] G.Zilizi.[42,¶]

1 I. Physikalisches Institut, RWTH, D-52056 Aachen, FRG[§]
III. Physikalisches Institut, RWTH, D-52056 Aachen, FRG[§]
2 National Institute for High Energy Physics, NIKHEF, and University of Amsterdam, NL-1009 DB Amsterdam, The Netherlands
3 University of Michigan, Ann Arbor, MI 48109, USA
4 Laboratoire d'Annecy-le-Vieux de Physique des Particules, LAPP,IN2P3-CNRS, BP 110, F-74941 Annecy-le-Vieux CEDEX, France
5 Institute of Physics, University of Basel, CH-4056 Basel, Switzerland
6 Louisiana State University, Baton Rouge, LA 70803, USA
7 Institute of High Energy Physics, IHEP, 100039 Beijing, China[△]
8 Humboldt University, D-10099 Berlin, FRG[§]
9 University of Bologna and INFN-Sezione di Bologna, I-40126 Bologna, Italy
10 Tata Institute of Fundamental Research, Bombay 400 005, India
11 Northeastern University, Boston, MA 02115, USA
12 Institute of Atomic Physics and University of Bucharest, R-76900 Bucharest, Romania
13 Central Research Institute for Physics of the Hungarian Academy of Sciences, H-1525 Budapest 114, Hungary[‡]
14 Massachusetts Institute of Technology, Cambridge, MA 02139, USA
15 INFN Sezione di Firenze and University of Florence, I-50125 Florence, Italy
16 European Laboratory for Particle Physics, CERN, CH-1211 Geneva 23, Switzerland
17 World Laboratory, FBLJA Project, CH-1211 Geneva 23, Switzerland
18 University of Geneva, CH-1211 Geneva 4, Switzerland
19 Chinese University of Science and Technology, USTC, Hefei, Anhui 230 029, China[△]
20 SEFT, Research Institute for High Energy Physics, P.O. Box 9, SF-00014 Helsinki, Finland
21 University of Lausanne, CH-1015 Lausanne, Switzerland
22 INFN-Sezione di Lecce and Universitá Degli Studi di Lecce, I-73100 Lecce, Italy
23 Los Alamos National Laboratory, Los Alamos, NM 87544, USA
24 Institut de Physique Nucléaire de Lyon, IN2P3-CNRS,Université Claude Bernard, F-69622 Villeurbanne, France
25 Centro de Investigaciones Energéticas, Medioambientales y Tecnologícas, CIEMAT, E-28040 Madrid, Spain[♭]
26 INFN-Sezione di Milano, I-20133 Milan, Italy
27 Institute of Theoretical and Experimental Physics, ITEP, Moscow, Russia
28 INFN-Sezione di Napoli and University of Naples, I-80125 Naples, Italy
29 Department of Natural Sciences, University of Cyprus, Nicosia, Cyprus
30 University of Nijmegen and NIKHEF, NL-6525 ED Nijmegen, The Netherlands
31 California Institute of Technology, Pasadena, CA 91125, USA
32 INFN-Sezione di Perugia and Universitá Degli Studi di Perugia, I-06100 Perugia, Italy
33 Carnegie Mellon University, Pittsburgh, PA 15213, USA
34 Princeton University, Princeton, NJ 08544, USA
35 INFN-Sezione di Roma and University of Rome, "La Sapienza", I-00185 Rome, Italy
36 Nuclear Physics Institute, St. Petersburg, Russia
37 University and INFN, Salerno, I-84100 Salerno, Italy
38 University of California, San Diego, CA 92093, USA
39 Dept. de Fisica de Particulas Elementales, Univ. de Santiago, E-15706 Santiago de Compostela, Spain
40 Bulgarian Academy of Sciences, Central Lab. of Mechatronics and Instrumentation, BU-1113 Sofia, Bulgaria
41 Center for High Energy Physics, Adv. Inst. of Sciences and Technology, 305-701 Taejon, Republic of Korea
42 University of Alabama, Tuscaloosa, AL 35486, USA
43 Utrecht University and NIKHEF, NL-3584 CB Utrecht, The Netherlands
44 Purdue University, West Lafayette, IN 47907, USA
45 Paul Scherrer Institut, PSI, CH-5232 Villigen, Switzerland
46 DESY-Institut für Hochenergiephysik, D-15738 Zeuthen, FRG
47 Eidgenössische Technische Hochschule, ETH Zürich, CH-8093 Zürich, Switzerland
48 University of Hamburg, D-22761 Hamburg, FRG
49 National Central University, Chung-Li, Taiwan, China
50 Department of Physics, National Tsing Hua University, Taiwan, China
§ Supported by the German Bundesministerium für Bildung, Wissenschaft, Forschung und Technologie
‡ Supported by the Hungarian OTKA fund under contract numbers T019181, F023259 and T024011.
¶ Also supported by the Hungarian OTKA fund under contract numbers T22238 and T026178.
♭ Supported also by the Comisión Interministerial de Ciencia y Tecnología.
♯ Also supported by CONICET and Universidad Nacional de La Plata, CC 67, 1900 La Plata, Argentina.
♮ Supported by Deutscher Akademischer Austauschdienst.
♢ Also supported by Panjab University, Chandigarh-160014, India.
△ Supported by the National Natural Science Foundation of China.

References

[1] T. Barnes, in Proceedings of the IXth International Workshop on Photon-Photon Collisions, (World Scientific, 1992), p. 263.

[2] C.R. Münz, Nucl. Phys. **A 609** (1996) 364.

[3] H.-W. Huang, C.-F. Qiao, and K.-T. Chao, Phys. Rev. **D 54** (1996) 2123.

[4] G.A. Schuler, F.A. Berends , and R. van Gulik, Nucl. Phys. **B 523** (1998) 423.

[5] Z.P. Li, F.E. Close, and T. Barnes, Phys. Rev. **D 43** (1991) 2161.

[6] W. Kwong *et al.*, Phys. Rev. **D 37** (1988) 3210.

[7] G.T. Bodwin, E. Braaten, and G.P. Lepage, Phys. Rev. **D 46** (1992) R1914.

[8] M. Consoli and J.H. Field, Phys. Rev. **D 49** (1994) 1293.

[9] M.L. Mangano and A. Petrelli, Phys. Lett. **B 352** (1995) 445.

[10] V.M. Budnev *et al.*, Phys. Rep. **15** (1974) 181.

[11] Particle Data Group, C. Caso *et al.*, Eur. Phys. J. **C3** (1998) 1.

[12] L.D. Landau, Dokl. Akad. Nauk. USSR **60** (1948) 207;
C.N. Yang, Phys. Rev. **77** (1950) 242.

[13] L3 Collab., B. Adeva *et al.*, Nucl. Inst. Meth. **A 289** (1990) 35;
M. Chemarin *et al.*, Nucl. Inst. Meth. **A 349** (1994) 345;
M. Acciarri *et al.*, Nucl. Inst. Meth. **A 351** (1994) 300;
G. Basti *et al.*, Nucl. Inst. Meth. **A 374** (1996) 293;
I.C. Brock *et al.*, Nucl. Inst. Meth. **A 381** (1996) 236;
A. Adam *et al.*, Nucl. Inst. Meth. **A 383** (1996) 342.

[14] T. van Rhee, Ph.D. thesis in preparation, University of Utrecht.

[15] F.L. Linde, Ph.D. thesis, University of Leiden, 1988, unpublished.

[16] A.D. Martin, M.G. Olsson, and W.J. Stirling, Phys. Lett. **147B** (1984) 203.

[17] G.A. Schuler, private communication.

[18] E760 Collab., T.A. Armstrong *et al.*, Phys. Rev. **D 48** (1993) 3037.

[19] The L3 detector simulation is based on GEANT version 3.15.
R. Brun *et al.*, GEANT 3, CERN-DD/EE/84-1 (Revised) 1987.

[20] ALEPH Collab., R. Barate *et al.*, Eur. Phys. J. **C4** (1998) 409.

[21] R704 Collab., C. Baglin *et al.*, Phys. Lett. **B 187** (1987) 191.

[22] TPC/2γ Collab., D.A. Bauer *et al.*, Phys. Lett. **B 302** (1993) 345.

[23] E760 Collab., T.A. Amstrong *et al.*, Phys. Rev. Lett. **70** (1993) 2988.

[24] CLEO Collab., J. Dominick *et al.*, Phys. Rev. **D 50** (1994) 4265.

[25] OPAL Collab., K. Ackerstaff *et al.*, Preprint CERN-EP/98-106, CERN, 1998.

Error source	$\Delta\Gamma_{\gamma\gamma}/\Gamma_{\gamma\gamma}$
Cut on E_γ	7%
Cut on $M(\ell^+\ell^-)$	11%
Trigger simulation	4%
Form factor	4%
Only $\|\lambda\| = 2$ formation	1%
Decay amplitudes	3%
Total systematic error	15%

Table 1: Summary of the contributions to the relative systematic error on the two-photon width.

Experiment	Production mechanism	$\Gamma_{\gamma\gamma}(\chi_{c2})$ (keV)
R704 [21]	$p\bar{p} \to \chi_{c2} \to \gamma\gamma$	$2.0^{+0.9}_{-0.7} \pm 0.3$
TPC/2γ [22]	$\gamma\gamma \to \chi_{c2} \to \gamma J$	$3.4 \pm 1.7 \pm 0.9$
E760 [23]	$p\bar{p} \to \chi_{c2} \to \gamma\gamma$	$0.32 \pm 0.08 \pm 0.05$
CLEO [24]	$\gamma\gamma \to \chi_{c2} \to \gamma J$	$1.08 \pm 0.30 \pm 0.26$
OPAL [25]	$\gamma\gamma \to \chi_{c2} \to \gamma J$	$1.76 \pm 0.47 \pm 0.37 \pm 0.15$
L3 (this analysis)	$\gamma\gamma \to \chi_{c2} \to \gamma J$	$1.02 \pm 0.40 \pm 0.15 \pm 0.09$
Prediction		
Barnes [1]		0.34 - 0.56
Münz [2]		0.44 ± 0.14
Huang *et al.* [3]		0.39 - 0.50
Schuler *et al.* [4]		0.28

Table 2: Summary of the published measurements and theoretical predictions of $\Gamma_{\gamma\gamma}(\chi_{c2})$. The R704 measurement has been updated using the current values [11] for $\Gamma_{\chi_{c2}}$ and $BR(\chi_{c2} \to p\bar{p})$.

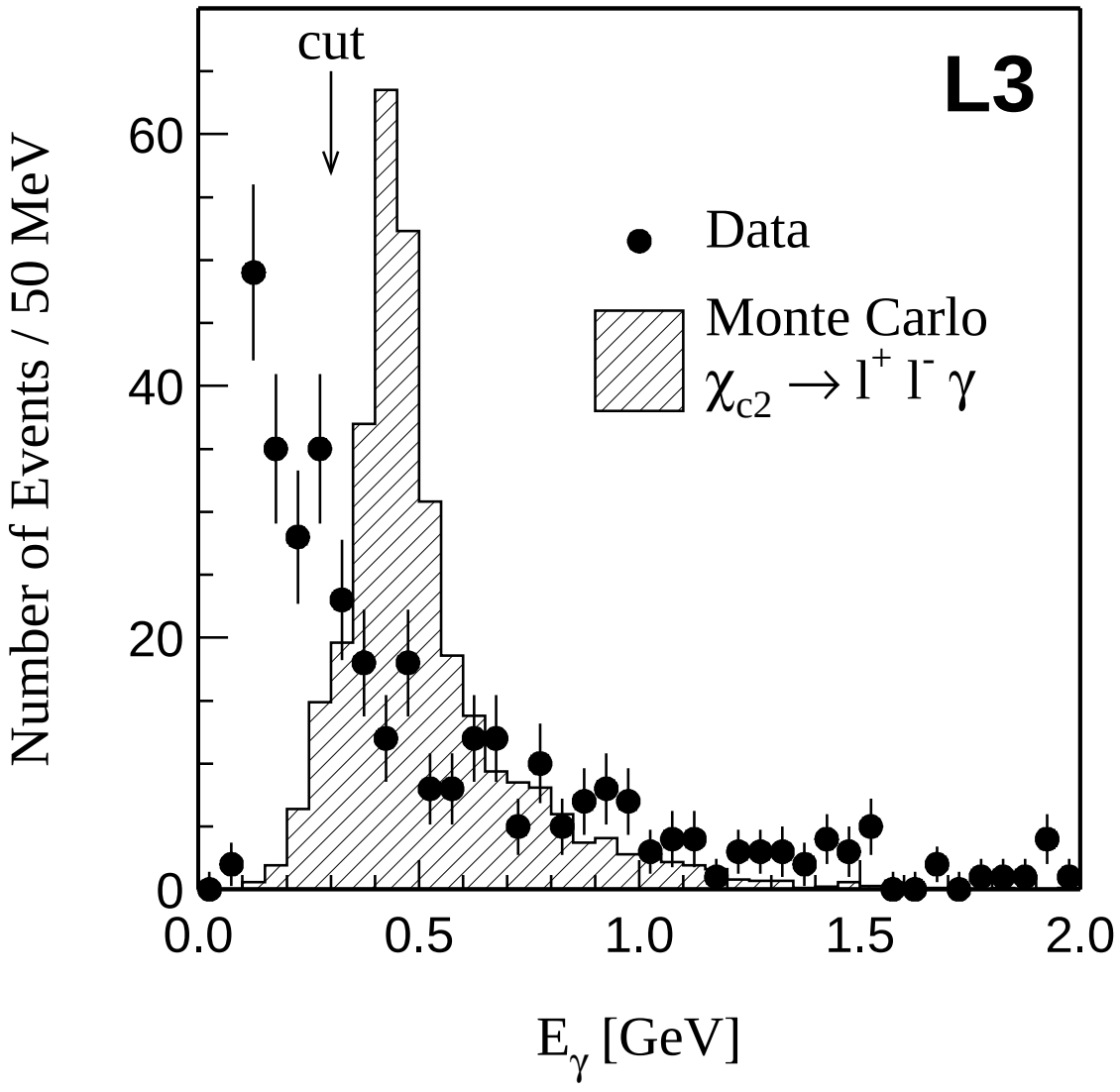

Figure 1: The photon energy E_γ for data (points with error bars) and Monte Carlo $\chi_{c2} \to \gamma$J, J $\to e^+e^-$ or $\mu^+\mu^-$ (histogram), after all other cuts have been applied. The normalisation of the Monte Carlo is arbitrary. The arrow indicates the cut on E_γ.

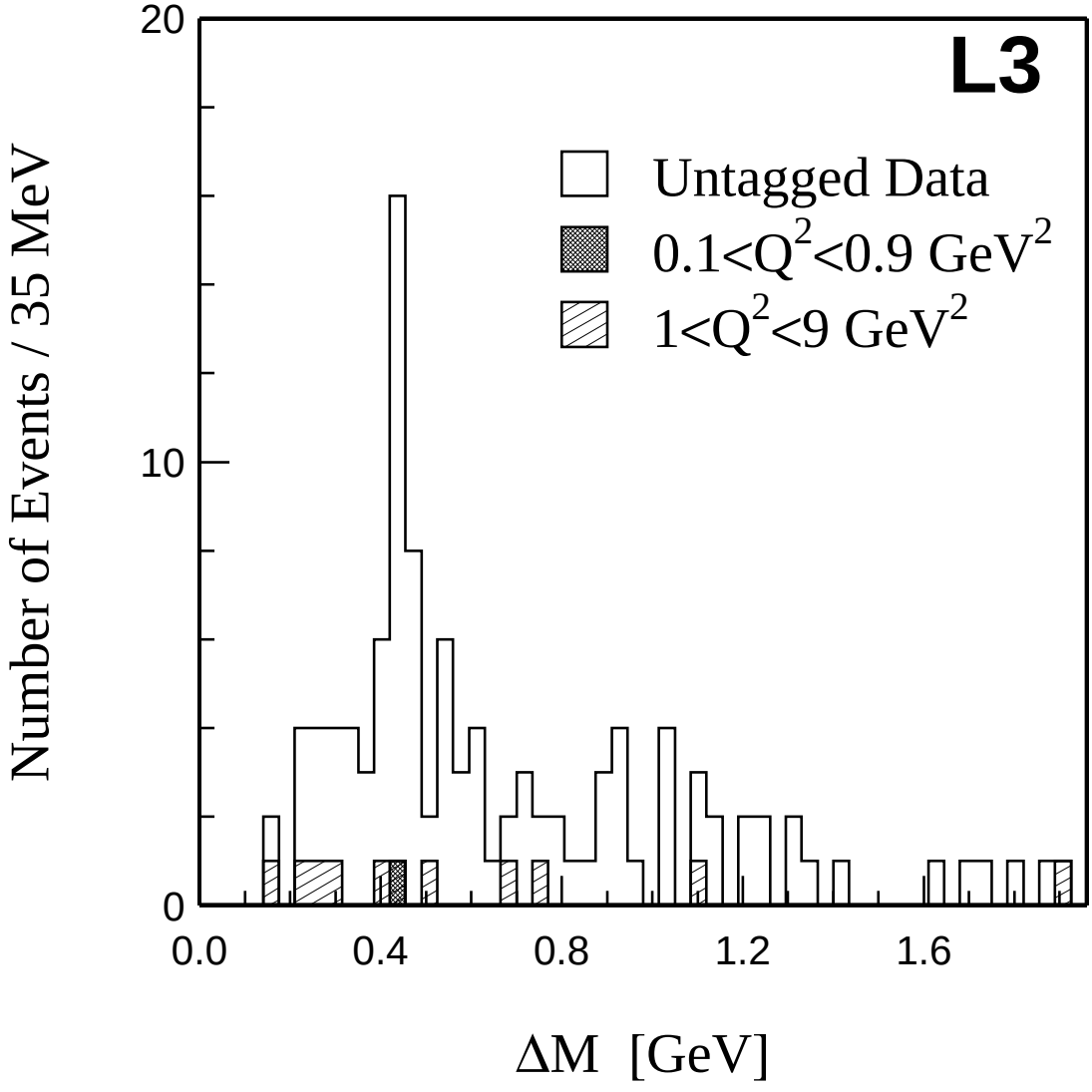

Figure 2: The mass difference $\Delta M = M(\ell^+\ell^-\gamma) - M(\ell^+\ell^-)$ for the total sample of selected LEP1 and LEP2 events. The hatched entries are single-tagged events for two different regions of Q^2, where $-Q^2$ is the invariant mass squared of the most virtual photon.

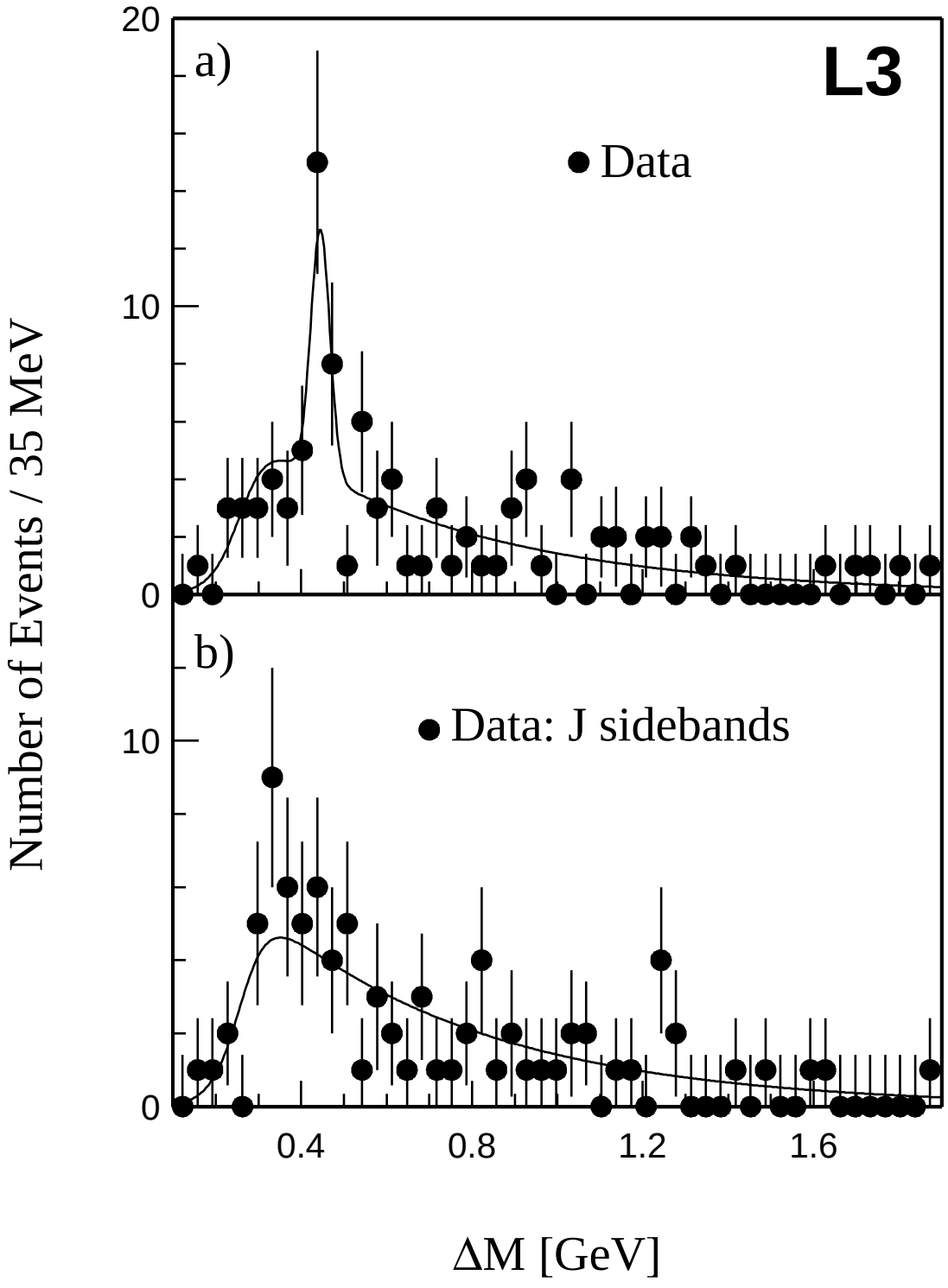

Figure 3: The distribution of the mass difference $\Delta M = M(\ell^+\ell^-\gamma) - M(\ell^+\ell^-)$, (a) for the selected data sample and (b) for the J sidebands. The curves show the signal and background functions, which have been determined in a simultaneous fit (see text).